Indian J. pure appl. Math., 32(6) : 931-942, June 2001

INTERACTION OF HORIZONTALLY POLARISED SH-WAVE WITH A GRIFFITH CRACK MOVING ALONG THE BIMATERIAL INTERFACE

R. K. PRAMANIK*, S. C. PAL** AND M. L. GHOSH*

*Department of Mathematics, University of North Bengal, District Darjeeling 734 430, West Bengal, India

**Department of Computer Application, University of North Bengal, District Darjeeling 734 430, West Bengal, India

[E-mail: scpal@dte.vsnl.net.in]

Scattering of horizontally polarised shear wave by a Griffith crack moving with uniform velocity along a bimaterial interface has been investigated. Using Fourier transform technique, the mixed boundary value problem has been reduced to the solution of a pair of dual integral equations. These equations are further reduced to a pair of coupled Fredholm integral equation of the second kind. The singular character of the dynamic stress near the crack tip has been examined and the expression for dynamic stress intensity factor has been derived. The dynamic stress intensity factors for several values of wave number, angle of incidence, crack speed and material constants have been depicted by means of graphs.

Key Words : Crack at Bimaterial Interface; Moving Crack; SH-Wave Diffraction; Stress Intensity Factor

1. INTRODUCTION

Scattering of elastic waves by a stationary or moving crack of finite width at the interface of two dissimilar elastic materials is important in view of its application in seismology as well as in fracture mechanics. The diffraction of Love waves by a stationary crack of finite width at the interface was investigated by Neerhoff[1]. Kuo[2] carried out analytical and numerical studies of transient response of an interfacial crack between two dissimilar orthotropic half spaces. Srivastava *et al.*[3] also derived the low frequency solution of the interaction of SH-wave by a Griffith crack at the interface of two bonded dissimilar elastic media.

In the case of cracks of finite size, moving with uniform velocity, loads, for mathematical simplicity, are usually assumed to be independent of time. However, in practice, structures are often required to sustain oscillating loads where the dynamic disturbances propagate through the elastic medium in the form of stress waves. The problem of diffraction of a plane harmonic polarized shear wave by a half-plane crack extended under antiplane strain was first studied by Jahanshahi[4]. Later Sih and Loeber[5] and Chen and Sih[6] also considered the problem of scattering of plane harmonic wave by a running crack of finite length. Recently, the high frequency solution of the problem of diffraction of the horizontally polarizes shear wave by a finite crack moving on a bimaterial interface has been investigated by Pal and Ghosh[7] using Wiener-Hopf technique.

In the present paper, we have investigated the low frequency solution of the scattering of plane SH-wave by a finite crack moving on bimaterial interface with uniform velocity. Using moving coordinate system and Fourier transform technique, the elastodynamic problem has been reduced to two pairs of dual integral equations. Following Sih and Loeber[5], the solution is then obtained in terms of a pair of coupled Fredholm integral equations. Finally the singular nature of the stress near

about the crack tip has been determined. The numerical values of dynamic stress intensity factor versus dimensionless wave number have been depicted by means of graphs for various parameters of material properties, crack speed and the angle of incidence.

2. Formulation of the Problem and its Solution

Let a plane crack of finite length $2a$ located at the interface of two bonded dissimilar semi-infinite elastic media be moving with a constant velocity V due to the incidence of plane harmonic SH-wave.

$$W_1^{(i)} = W_0 \exp[-i\{\Lambda_1 (X\cos\theta_1 + Y\sin\theta_1) + \Omega T\}], \quad \ldots (2.1)$$

where W_0 is the wave amplitude, Λ_1 wave number, $\Omega (= \Lambda_1 C_1)$ circular frequency, $(\pi/2 - \theta_1)$ angle of incidence and C_1 is the shear wave velocity in the upper medium denoted by (1).

The crack lies in XZ plane with Z axis directed parallel to the edge of the crack with respect to the rectangular coordinate system (X, Y, Z) as shown in Fig. 1.

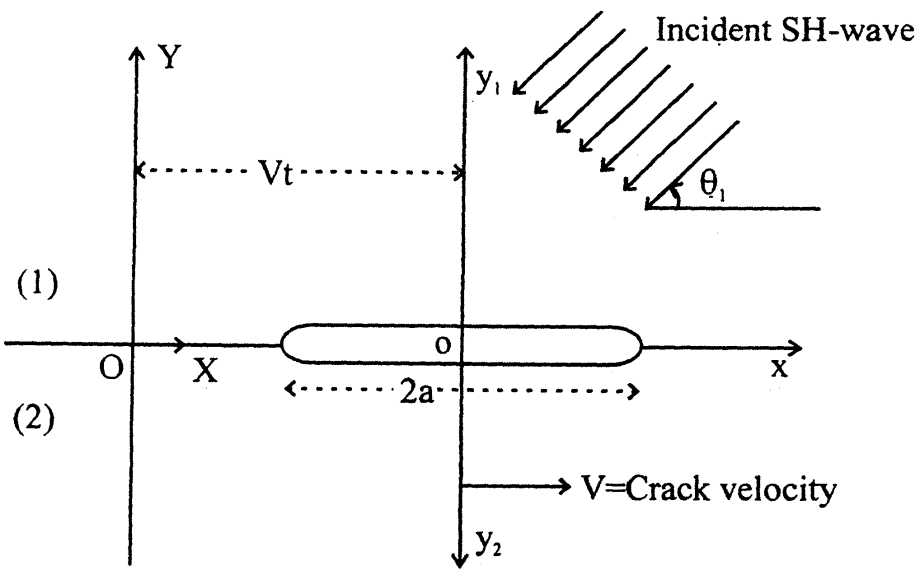

FIG. 1. Moving interface crack

We assume that the displacement and the stress due to scattered fields are

$$W_j = W_j(X, Y)\, e^{-i\Omega T} \quad \ldots (2.2)$$

and

$$(\tau_{XZ})_j = \mu_j \frac{\partial W_j}{\partial X} \text{ and } (\tau_{YZ})_j = \mu_j \frac{\partial W_j}{\partial Y} \quad \ldots (2.3)$$

where the subscripts $j = 1, 2$ refer to the upper and lower half plane respectively and T denotes time.

The equations of SH wave motion in either elastic half spaces are given by

$$\frac{\partial^2 W_j}{\partial X^2}+\frac{\partial^2 W_j}{\partial Y^2}=\frac{1}{C_j^2}\frac{\partial^2 W_j}{\partial T^2},\ (j=1,2) \qquad ...(2.4)$$

where $C_j=\sqrt{\frac{\mu_j}{\rho_j}}$ is the shear wave velocity and μ_j, ρ_j and coefficient of rigidity and material density respectively. Without any loss of generality we further assume that $C_1 > C_2$.

Due to the incident wave given in eq. (2.1), the reflected and transmitted wave in the absence of the crack may be written as

$$W_1^{(R)}=A\exp\ [-\ i\ \{\Lambda_1\ (X\cos\theta_1 - Y\sin\theta_1)+\Omega T\}]$$

and
$$W_2^{(T)}=B\exp\ [-\ i\ \{\Lambda_2\ (X\cos\theta_2 - Y\sin\theta_2)+\Omega T\}] \qquad ...\ (2.5)$$

where
$$A=\frac{\mu_1\Lambda_1\sin\theta_1-\mu_2\Lambda_2\sin\theta_2}{\mu_1\Lambda_1\sin\theta_1+\mu_2\Lambda_2\sin\theta_2}W_0,\ B=\frac{2\mu_1\Lambda_1\sin\theta_1}{\mu_1\Lambda_1\sin\theta_1+\mu_2\Lambda_2\sin\theta_2}W_0 \qquad ...\ (2.6)$$

with
$$\Lambda_1\cos\theta_1=\Lambda_2\cos\theta_2.$$

A, B are the reflected and transmitted wave amplitudes, Λ_j wave number, $\Omega\ (=\Lambda_j C_j)$ the circular frequency and $(\pi/2-\theta_1)$ and $(\pi/2-\theta_2)$ the angles of incidence and refraction respectively.

A set of moving coordinate system (x, y_j, z, t) moving along with the crack at a constant velocity V in X-direction is introduced in accordance with

$$x=X-Vt,\ y_j=s_j Y,\ z=Z,\ t=T, \qquad ...\ (2.7)$$

where $s_j^2=1-M_j^2$ and $M_j=V/C_j$ is the Mach number.

$M_j<1$, since the crack is assumed to travel at subsonic speed.

In terms of moving co-ordinate system (x, y_j, t) equation (2.4) becomes

$$\frac{\partial^2 W_j}{\partial x^2}+\frac{\partial^2 W_j}{\partial y_j^2}+\frac{1}{C_j^2 s_j^2}\frac{\partial}{\partial t}\left[2V\frac{\partial W_j}{\partial x}-\frac{\partial W_j}{\partial t}\right]=0. \qquad ...\ (2.8)$$

Further, referred to moving coordinate system, incident and reflected and transmitted wave given by eqs. (2.1) and (2.5) take the following form,

$$W_1^{(i)}=W_0\,e^{-i\omega t}\exp\left[-i\Lambda_1\left(x\cos\theta_1+\frac{y_1}{s_1}\sin\theta_1\right)\right],$$

$$W_1^{(R)}=Ae^{-i\omega t}\exp\left[-i\Lambda_1\left(x\cos\theta_1-\frac{y_1}{s_1}\sin\theta_1\right)\right],$$

and $$W_2^{(T)} = Be^{-i\omega t} \exp\left[-i\Lambda_2 \left(x\cos\theta_2 + \frac{y_2}{s_2}\sin\theta_2 \right) \right], \quad \text{... (2.9)}$$

where $$\omega = \Omega\alpha \text{ and } \alpha = (1 + M_1\cos\theta_1) = (1 + M_2\cos\theta_2). \quad \text{... (2.10)}$$

It is convenient to write the solution of the eq. (2.8) in the form

$$W_j(x, y_j, t) = W_j(x, y_j)\, e^{-i\omega t} = w_j(x, y_j) \exp[i(\lambda_j M_j x - \omega t)] \quad \text{... (2.11)}$$

where $$\lambda_j = \frac{\Lambda_j}{s_j}\alpha. \quad \text{... (2.12)}$$

Substitution of eq. (2.11) into eq. (2.8) yields the Helmhlotz eq. governing w_j

$$\frac{\partial^2 w_j}{\partial x^2} + \frac{\partial^2 w_j}{\partial y_j^2} + \lambda_j^2 w_j = 0. \quad \text{... (2.13)}$$

The solution of eq. (2.13) can be written as

$$w_j(x, y_j) = \frac{1}{2\pi}\int_{-\infty}^{\infty} A_j(\xi)\, e^{-i\xi x - \beta_i |y_j|}\, d\xi \quad \text{... (2.14)}$$

where $$\beta_j = \sqrt{\xi^2 - \lambda_j^2}. \quad \text{... (2.15)}$$

From eqs. (2.11) and (2.14) the displacement components of the diffracted field can be expressed as

$$W_j(x, y_j) = \frac{1}{2\pi}\int_{P-\infty}^{\infty} B_j(\xi)\, e^{-i\xi x - \gamma_j |y_j|}\, d\xi, \quad \text{... (2.16)}$$

where $$\gamma_j = \sqrt{(\xi + \lambda_j M_j)^2 - \lambda_j^2}, \; B_j(\xi) = A_j(\xi + \lambda_j M_j). \quad \text{... (2.17)}$$

The unknown quantities $B_1(\xi)$ and $B_2(\xi)$ are to be determined from the following boundary conditions

$$\mu_1 s_1 \frac{\partial W_1}{\partial y_1} = \mu_2 s_2 \frac{\partial W_2}{\partial y_2} \text{ for all } x, y_j = 0$$

$$W_1 = W_2; \; |x| > a; \; Y_j = 0$$

$$\frac{\partial W_1}{\partial Y_1} + \frac{\partial W_1^{(i)}}{\partial y_1} + \frac{\partial W_1^{(R)}}{\partial y_1} = 0; \; |x| < a; \; y_j = 0. \quad \text{.. (2.18)}$$

From the first boundary condition of eqs. (2.18) one obtains

$$\mu_1 s_1 \gamma_1 B_1(\xi) + \mu_2 s_2 \gamma_2 B_2(\xi) = 0. \qquad \ldots (2.19)$$

The other two boundary conditions yield the following dual integral equations

$$\frac{1}{2\pi} \int_{-\infty}^{\infty} P_1(\xi) e^{-i\xi x} d\xi = 0;\ |x| > a, y_j = 0$$

and

$$\frac{1}{2\pi} \int_{-\infty}^{\infty} E_1(\xi) P_1(\xi) e^{-i\xi x} d\xi = -D_1 e^{-i\Lambda_1 x \cos\theta_1};\ |x| < a, \qquad \ldots (2.20)$$

where

$$P_1(\xi) = \frac{s_1 \mu_1 \gamma_1 + s_2 \mu_2 \gamma_2}{\gamma_2} B_1(\xi), \qquad \ldots (2.21)$$

$$E_1(\xi) = \frac{\gamma_1 \gamma_2}{s_1 \mu_1 \gamma_1 + s_2 \mu_2 \gamma_2} \qquad \ldots (2.22)$$

and

$$D_1 = \left(\frac{2\mu_2 \Lambda_2 \sin\theta_2}{\mu_1 \Lambda_1 \sin th\eta_1 + \mu_2 \Lambda_2 \sin\theta_2} \right) \frac{i\Lambda_1 \sin\theta_1}{s_1} W_0 \qquad \ldots (2.23)$$

Eq. (2.20) can further be reduced to two sets of dual integral equations. They are

$$\frac{2}{\pi} \int_0^{\infty} P_{1e}(\xi) \cos(\xi x) d\xi = 0;\ |x| > a, y_j = 0;$$

$$\frac{2}{\pi} \int_0^{\infty} E_{1e}(\xi) P_{1e}(\xi) \cos(\xi x) d\xi$$

$$= -2D_1 \cos(\Lambda_1 x \cos\theta_1) - 2\pi \int_0^{\infty} E_{1o}(\xi) P_{1o}(\xi) \cos(\xi x) d\xi;\ |x| < a. \qquad \ldots (2.24)$$

and

$$\frac{2}{\pi} \int_0^{\infty} P_{1o}(\xi) \sin(\xi x) d\xi = 0;\ |x| > a, y_j = 0;$$

$$\frac{2}{\pi} \int_0^{\infty} E_{1e}(\xi) P_{1o}(\xi) \sin(\xi x) d\xi$$

$$= -2D_1 \sin(\Lambda_1 x \cos\theta_1) - \frac{2}{\pi} \int_0^{\infty} e_{1o}(\xi) P_{1e}(\xi) \sin(\xi x) d\xi;\ |x| < a, \qquad \ldots (2.25)$$

where $$P_1(\xi) = \frac{1}{2}[P_1(\xi) + P_1(-\xi)] + \frac{1}{2}[P_1(\xi) - P_1(-\xi)] = P_{1e}(\xi) + P_{1o}(\xi)$$

$$E_1(\xi) = \frac{1}{2}[E_1(\xi) + E_1(-\xi)] + \frac{1}{2}[E_1(\xi) - E_1(-\xi)] = E_{1e}(\xi) + E_{1o}(\xi). \quad \text{... (2.26)}$$

The problems in eqs. (2.24) and (2.25) are respectively even and odd in x. The solution procedure described in [8] can be used to solve eqs. (2.24) and (2.25) and the result is a coupled Fredholm integral equation of the second kind. In order to solve eqs. (2.24) and (2.25) it is assumed that

$$P_{1e}(\xi) = \frac{\pi D_1 a^2}{K} \int_0^1 \sqrt{s}\, \Delta_1(s)\, J_0(a\,\xi\, s)\, ds \quad \text{... (2.27)}$$

and $$P_{1o}(\xi) = \frac{\pi D_1 a}{K\xi}\left[\int_0^1 \sqrt{s}\, \Gamma_1(s)\, J_0(a\,\xi\, s)\, ds - i\,\Omega_1(1)\, J_0(a\,\xi)\right] \quad \text{... (2.28)}$$

where $$i\,\Omega_1(1) = \int_0^1 \sqrt{s}\, \Gamma_1(s)\, ds. \quad \text{... (2.29)}$$

Substitution of eqs. (2.27) and (2.28) in eqs. (2.24) and (2.25) yields the following coupled integral equations for the determination of $\Delta_1(s)$ and $\Gamma_1(s)$

$$\Delta_1(s) - \int_0^1 \Delta_1(\eta)\, M_1(s,\eta)\, d\eta - \int_0^1 \Gamma_1(\eta)\,[N_1(s,\eta) - \sqrt{\eta}\, N_1(s,1)]\, d\eta$$

$$= \sqrt{s}\, J_0(\Lambda_1\, as\cos\theta_1);$$

$$\Gamma_1(s) - \int_0^1 \Delta_1(\eta)\left\{L_1(s,\eta) - \frac{K'a}{K} M_1(s,\eta)\right\} d\eta +$$

$$+ \int_0^1 \Gamma_1(\eta)\left\{\frac{K'a}{K}[N_1(s,\eta) - \sqrt{\eta}\, N_1(s,1)] - [M_1(s,\eta) - \sqrt{\eta}\, M_1(s,1)]\right\} d\eta$$

$$= \sqrt{s}\left(\Lambda_1 a\cos\theta_1 - \frac{K'a}{K}\right) J_0(\Lambda_1\, as\cos\theta_1); \quad \text{... (2.30)}$$

where $$K = -\frac{1}{(s_1\mu_1 + s_2\mu_2)}, \quad \text{... (2.31)}$$

$$K' = -\frac{(\lambda_1 M_1 s_2\mu_2 + \lambda_2 M_2 s_1\mu_1)}{(s_1\mu_1 + s_2\mu_2)^2}, \quad \text{... (2.32)}$$

$$M_1(s,\eta)=\frac{\sqrt{s\,\eta}}{K}\int_0^\infty \xi H_{1e}(\xi/a)\,J_0(\xi\,\eta)\,J_0(\xi s)\,d\xi, \qquad \ldots (2.33)$$

$$N_1(s,\eta)=\frac{\sqrt{s\,\eta}}{K}\int_0^\infty \frac{a}{\xi}E_{1o}(\xi/a)\,J_0(\xi\,\eta)\,J_0(\xi s)\,d\xi, \qquad \ldots (2.34)$$

and

$$L_1(s,\eta)=\frac{\sqrt{s\,\eta}}{K}\int_0^\infty a\,\xi H_{1o}(\xi/a)\,J_0(\xi\,\eta)\,J_0(\xi s)\,d\xi \qquad \ldots (2.35)$$

in which $H_{1e}(\xi)$ and $H_{1o}(\xi)$ are defined as

$$H_{1e}(\xi)=\frac{E_{1e}(\xi)}{\xi}+K\to O(\xi^{-2}) \text{ as } \xi\to\infty$$

and

$$H_{1o}(\xi)=E_{1o}(\xi)+K'\to O(\xi^{-2}) \text{ as } \xi\to\infty. \qquad \ldots (2.36)$$

3. Stress Intensity Factor

Since the condition of the crack propagation is controlled by the stresses near the crack tips, we are mainly interested in determining the singular behaviour of the stress field near the crack tips.

With the aid of the eqs. (2.16) and (2.21) the stress in medium 1 can be written as

$$(\tau_{yz})_1=\mu_1 s_1\frac{\partial W_1}{\partial y_1}=-\frac{\mu_1 s_1}{2\pi}\int_{-\infty}^{\infty}E_1(\xi)\,P_1(\xi)\,e^{-i\xi x-\gamma_1 y_1}\,d\xi. \qquad \ldots (3.1)$$

For an examination of the singular behaviour of the stress near the crack tip ($x=\pm a$) it is sufficient to consider the dominating terms in the integrand of the integral (3.1) as $|\xi|\to\infty$.

Accordingly near the crack tip

$$[(\tau_{yz})_1]_{\text{at crack tip}} = -\frac{s_1\mu_1}{\pi(s_1\mu_1+s_2\mu_2)}\times$$

$$\times\left[\int_0^\infty \xi e^{-\xi y_i}P_{1e}\cos(\xi x)\,d\xi - i\int_0^\infty \xi e^{-\xi y_1}P_{1o}(\sin(\xi x)\,d\xi\right]. \qquad \ldots (3.2)$$

Further as $|x|\to\infty$

$$P_{1e}(\xi)=\frac{\pi D_1 a}{K\xi}\Delta_1(1)\,J_1(a\,\xi)+\ldots..$$

and

$$P_{1o}(\xi)=\frac{i\pi D_1 a}{K\xi}\Omega_1(1)\,J_0(a\,\xi)+\ldots.. \qquad \ldots (3.3)$$

Substituting the asymptotic expression of $P_{1e}(\xi)$ and $P_{1o}(\xi)$ as given by eq. (3.3) in equation (3.2) the singular stress field around $x = a$, $y = 0$ is obtained as

$$[(\tau_{yz})_1]_{x=a,\,y=0} = -\frac{\mu_1 s_1 D_1 \sqrt{a}}{\sqrt{2r}} \{\Omega_1(1) + \Delta_1(1)\} f(s_1) + O(1)$$

$$= \frac{\sigma_1 \sqrt{a}}{\sqrt{2r}} \left[\frac{\mu_1 \sin\theta_2}{\mu_1 + \mu_2 \cot\theta_1 \tan\theta_2} (\Omega_1(1) + \Delta_1(1)) \right] f(s_1) + O(1) \quad \ldots (3.4)$$

where $$f^2(s_1) = \frac{\sec\Phi}{2} (1 + s_1^2 \tan^2\Phi)^{-1/2} + (1 + s_1^2 \tan^2\Phi)^{-1}] \quad \ldots (3.5)$$

$$r = \sqrt{(x-a)^2 + y^2},\ \Phi = \tan^{-1}\left(\frac{y}{x-a}\right) \quad \ldots (3.6)$$

and $$\sigma_1 = -2i\mu_2 A_2 W_0. \quad \ldots (3.7)$$

Dynamic stress intensity factor K_1 is defined by

$$K_1 = \sigma_1 \sqrt{a} \left[\frac{\mu_1 \sin\theta_2}{\mu_1 + \mu_2 \cot\theta_1 \tan\theta_2} (\Phi_1(1) + \Delta_1(1)) \right]. \quad \ldots (3.8)$$

While studying the dynamic crack propagation the determination of stress intensity factor is important because it supplies useful information regarding the rate at which elastic and kinetic energies are released by the propagating crack.

4. Numerical Results and Discussion

Numerical results have been calculated to plot normalized stress intensity factor $|K_1/(\sigma_1\sqrt{a})|$ at the crack tip $x = a$, $y = 0$ versus the normalized wave number $\Lambda_1 a$ for different values of the Mach number M_1 and the angle of incidence for the following sets of materials :

First Set

Steel : $\rho_1 = 7.6$ gm/cm^3, $\mu_1 = 8.32 \times 10^{11}$dyne/cm^2

Aluminium : $\rho_2 = 2.7$ gm/cm^3, $\mu_2 = 4.5 \times 10^{11}$ dyne/cm^2

Second Set

Wrough iron : $\rho_1 = 7.8$ gm/cm^3, $\mu_1 = 7.7 \times 10^{11}$ dyne/cm^2

Copper : $\rho_2 = 8.96$ gm/cm^3, $\mu_2 = 4.5 \times 10^{11}$ dyne/cm^2

The numerical results have been obtained for low frequencies. The case $M_1 = 0$ corresponds to the stationary crack solution. It is found that by increasing the crack speed, the dimensionless stress intensity factor $|K_1/(\sigma_1\sqrt{a})|$ decreases with the normalized wave number $\Lambda_1 a$. It is interesting to note that as the velocity of the crack increases, the picks of the curves decreases in magnitude and occur at lower values of $\Lambda_1 a$ (Figs. 2-7).

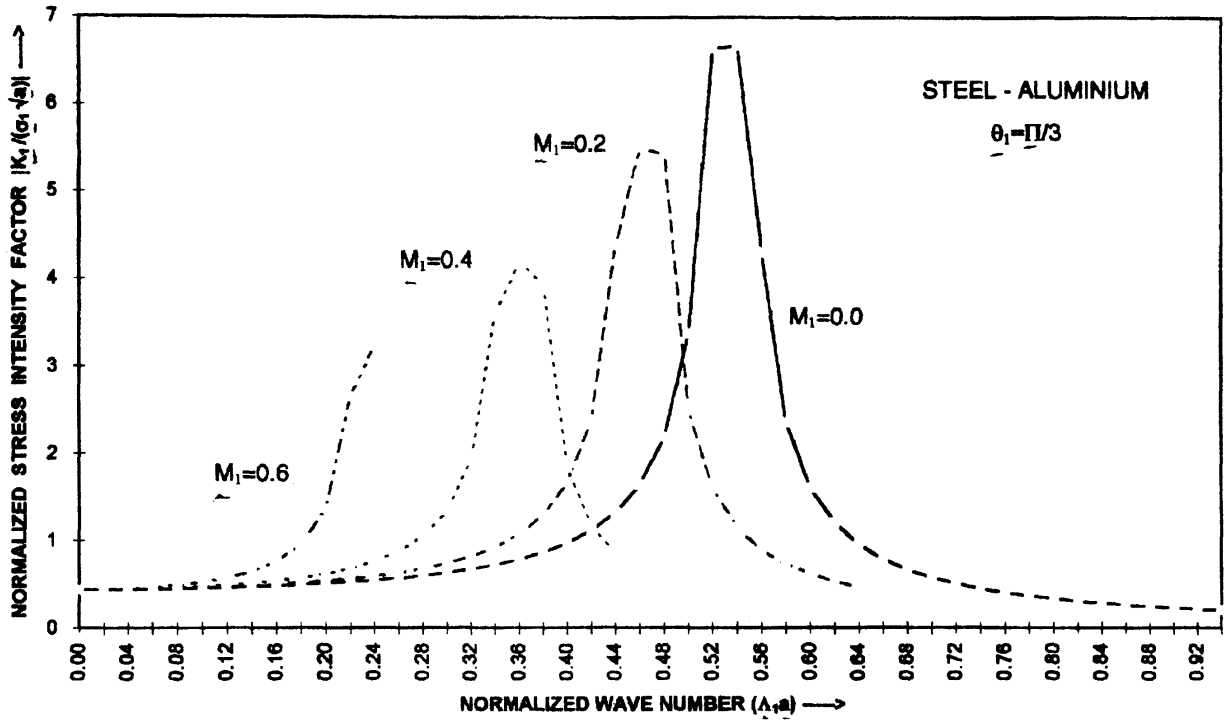

FIG. 2. Stress intensity factor vs wave number.

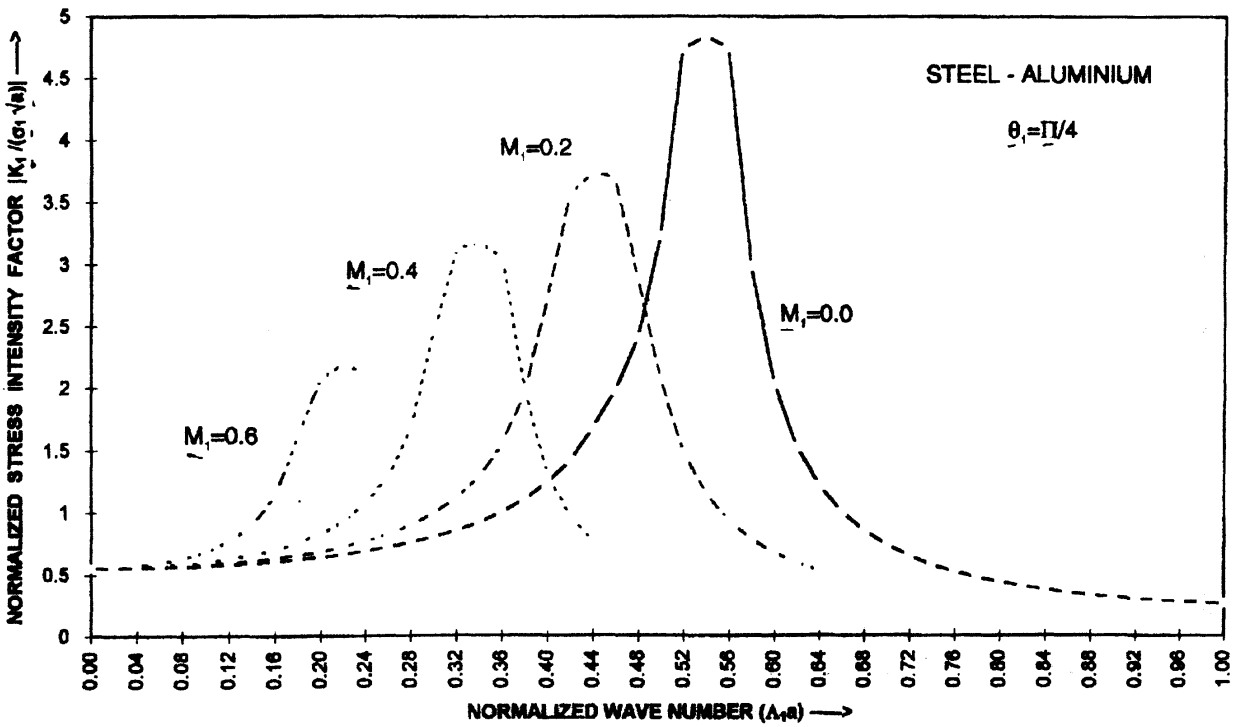

FIG. 3. Stress intensity factor vs wave number.

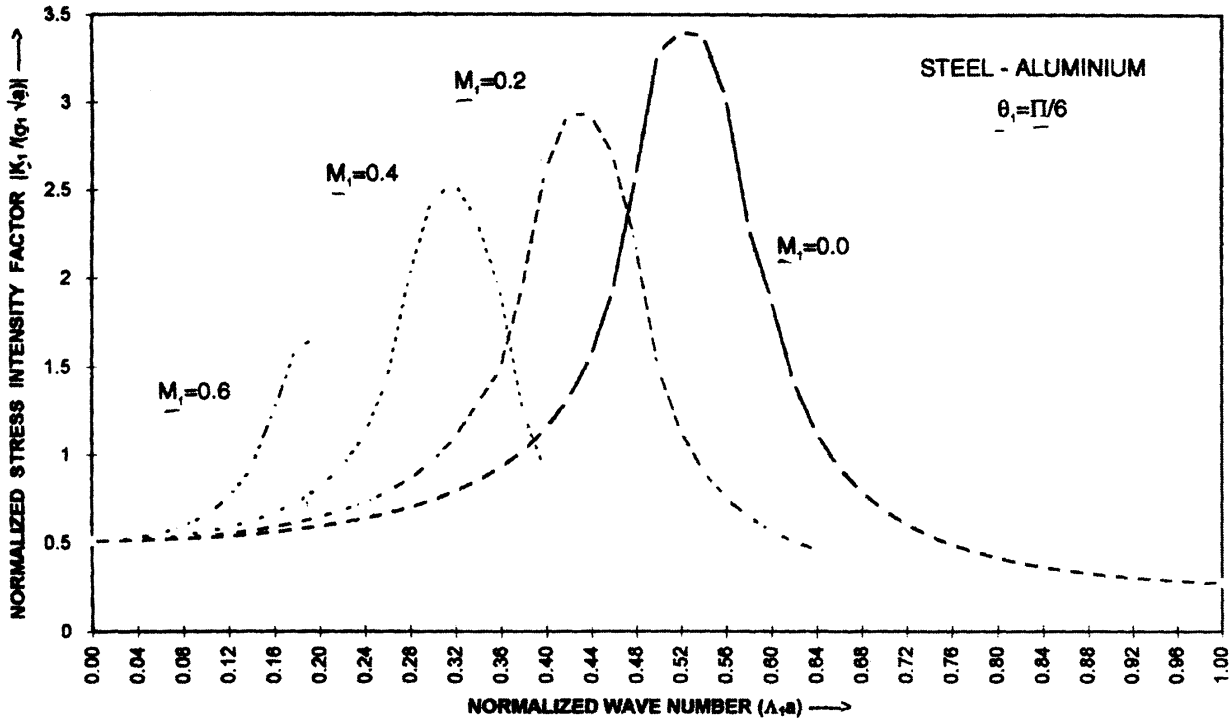

FIG. 4. Stress intensity factor vs wave number.

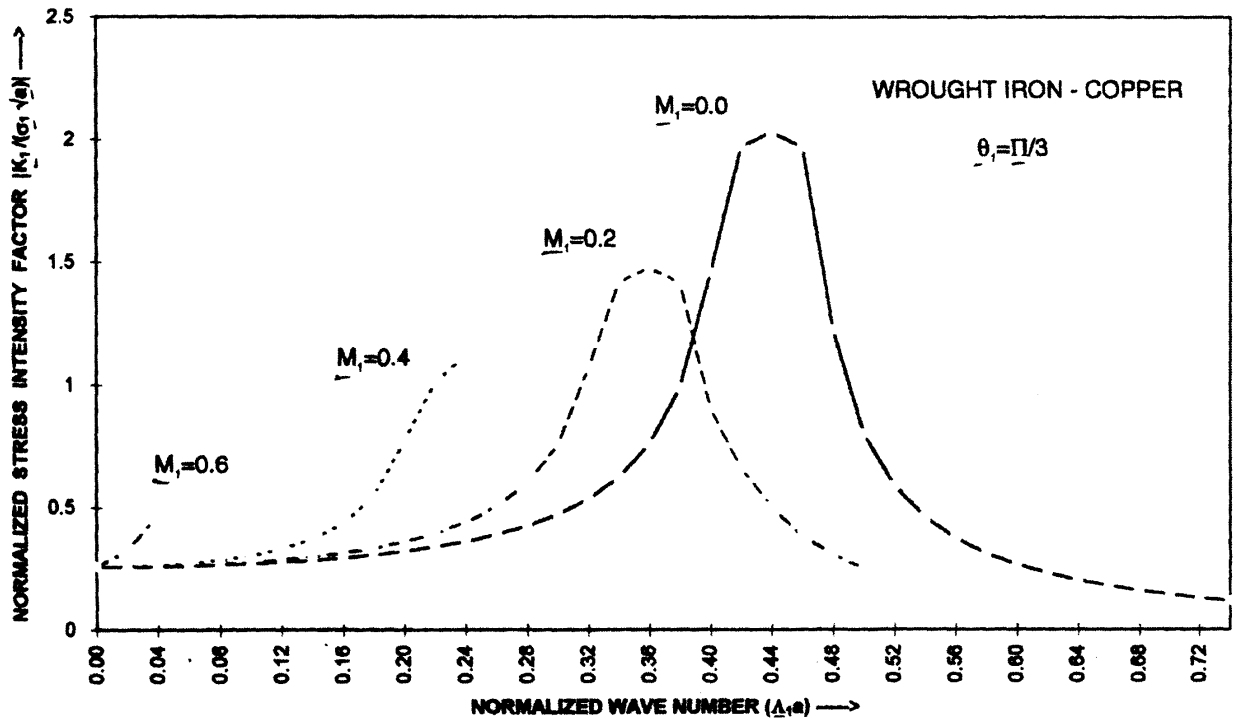

FIG. 5. Stress intensity factor vs wave number

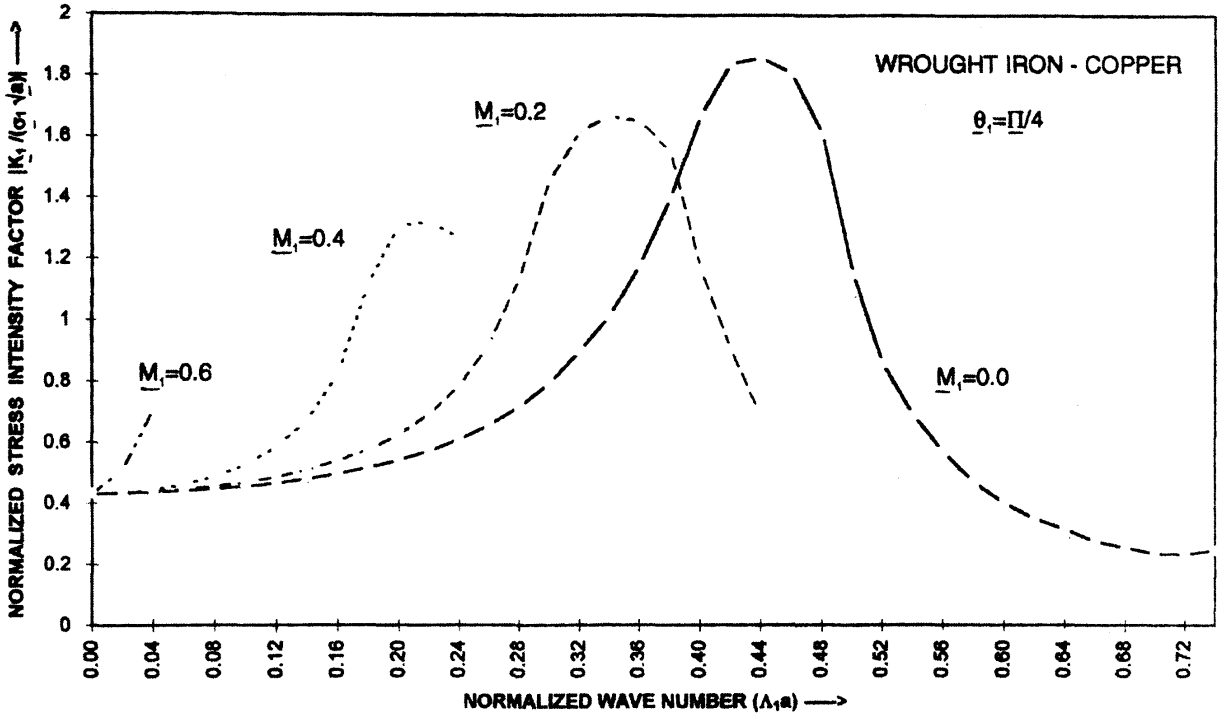

FIG. 6. Stress intensity factor vs wave number

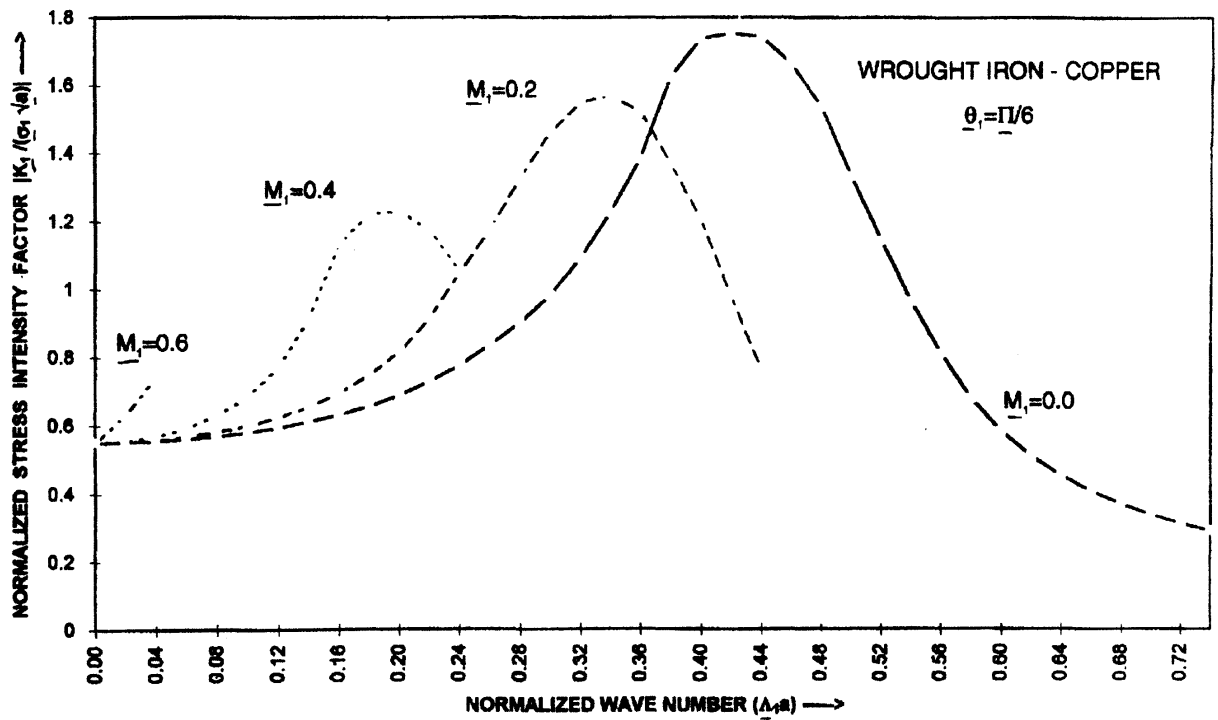

FIG. 7. Stress intensity factor vs wave number.

For both the pair of solids, graphs of stress intensity factor versus normalized wave number ($\Lambda_1 a$) have been plotted for the angles $\theta_1 = \pi/3$, $\theta_1 = \pi/4$, and as well as $\theta_1 = \pi/6$. It is also found that for a given pair of materials and for a given Mach number, the peak values of the stress intensity factors decrease with the decrease in the values of θ_1.

REFERENCES

1. F. L. Neerhoff, *Appl. Sci. Res.* **35** (1979) 265-315.
2. A. Y. Kuo, *J. appl. Mech.*, **51** (1984) 71-76.
3. K. N. Srivastava, R. M. Palaiya and D. S. Karaulia, *Int. J. Fracture.*, **16** (1980) 349-58.
4. A. Jahanshahi, *J. appl. Mech.*, **34** (1967) 100-103.
5. G. C. Sih and J. F. Loeber, *J. appl. Mech.*, **37** (1970) 324-30.
6. E. P. Chen and G. C. Sih, *J. appl. Mech.*, **42** (1975) 704-11.
7. S. C. Pal and M. L. Ghosh, *Engng. Fracture Mech.*, **45** (1993) 107-18.
8. G. C. Sih and J. F. Loeber, *Q. appl. Math.* **27** (1969) 193-203.